Microsolvation of Cationic Dimers in 4 He Droplets: Geometries of (He) N (A = Li, Na, K) from Optimized Energies †

6 AUTHORS, INCLUDING:

Emanuele Coccia
Pierre and Marie Curie University - Paris 6
22 PUBLICATIONS   220 CITATIONS

SEE PROFILE

David López-Durán
Spanish National Research Council
32 PUBLICATIONS   285 CITATIONS

SEE PROFILE

Enrico Bodo
Sapienza University of Rome
111 PUBLICATIONS   1,534 CITATIONS

SEE PROFILE

Franco A Gianturco
Sapienza University of Rome
448 PUBLICATIONS   6,201 CITATIONS

SEE PROFILE

Microsolvation of cationic dimers in ^{4}He droplets: geometries of A_2^+(He)$_N$ (A=Li,Na,K) from optimized energies.

F. Marinetti,[1] Ll. Uranga-Piña,[2] E. Coccia,[1] D.
López-Durán,[3] E. Bodo,[1] and F. A. Gianturco[1, *]

[1]*Department of Chemistry, The University of Rome La Sapienza, Rome, Italy.*

[2]*Department of Theoretical Physics, Physics Faculty, University of Havana, Cuba.*

[3]*Instituto de Matemáticas y Física Fundamental (CSIC), Madrid, Spain.*

Ab initio computed interaction forces are employed in order to describe the microsolvation of the A_2^+($^2\Sigma$) (A=Li,Na,K) molecular ion in ^{4}He clusters of small variable size. The minimum energy structures are obtained by performing energy minimization based on a genetic algorithm approach. The symmetry features of the collocation of solvent adatoms around the dimeric cation are analyzed in detail, showing that the selective growth of small clusters around the two sides of the ion during the solvation process is a feature common to all three dopants.

I. INTRODUCTION

The characterization of the structures and energetics of atomic and molecular aggregates is a current challenge of both theoretical and experimental research directed to attaining accurate descriptions of their nanoscopic properties. Weakly bound clusters of variable size, especially those involving helium and other noble gas atoms, represent an ideal testing ground for a large number of theoretical and computational approaches [1, 2, 3, 4, 5]: this is consequence of the fact that the accurate knowledge of the relevant intermolecular forces between the solvent atoms and the dopants present in the cluster is an important prerequisite for the structural calculations and therefore fairly simple components provide ideal model systems for the analysis of the influence of intermolecular interactions on the cluster properties [6, 7, 8].

In the case of weak dispersion interactions, the ground state configuration is responsible

*Corresponding author: fa.gianturco@caspur.it. Fax: +39-06-4991.3305.

for most of the microsolvation effects on chemical species and determines the outcome of possible chemical processes, which can in turn be used to help the synthesis of new molecules and isomers [9]. For noble gas atoms this has become an active area of research since, among them only the chemical properties of krypton are fairly understood. Extensive theoretical analysis of the bonding in compounds involving noble gases has been successful in that even some new molecules have been predicted through theory [10].

From the experimental point of view, atomic or molecular impurities embedded in noble gas clusters act as cromophoric units, allowing their spectroscopic investigation. Information about the structure of the cluster follows from the comparison between the results of measurements in the cluster and the isolated cromophore spectroscopy. Such an approach makes possible the evaluation of the effects of geometric modifications and of the solvent atoms vibrations on the local excitation spectra of the impurity. Doped helium clusters present some additional interesting features like the rapid heat transport generated inside the complex to the surface: due to such cooling, the He clusters are ideal candidates for low temperature chemistry studies since the density of states accessible to guest molecules is significantly reduced, minimizing the complexity of the system especially from the theoretical point of view. Helium droplets provide weakly-interacting, low temperature environments suitable for studying the evolution of molecular properties as the size of the cluster increases in a controlled fashion. It allows to establish a continuous bridge between the structural properties, energetics and chemical reaction dynamics in isolated molecules and those of condensed phase. Furthermore, the possibility to understand, at the microscopic level, the solvation process of an ionic impurity has also motivated a large number of theoretical and experimental research on ionic clusters involving noble gas atoms. Impurities like positive ions form a region of increased density due to electrostriction, leading to a larger local density of the He adatoms and to the formation of short-range order. This is known as the snowball model [11] and has been widely used in the interpretation of experimental data since this phenomenological picture explains the low mobility of a positive ions observed in experiment as compared with that of neutral species [12]. Therefore, positive ions are surrounded by many He atoms that are strongly compressed as a result of electrostriction, so that the resulting core is thought to lead to solid-like structures [13, 14], i.e. to a *snowball*. More specifically, the analogy with a *snowball* indicates the existence of some compact microstructure surrounded by a more liquid-like shell of less strongly localized ^{4}He adatoms

until the next solid-like configuration is formed.

For various doped helium clusters, numerically converged calculations of their structures and energies has been performed by Variational Monte Carlo (VMC) [15] and Diffusion Monte Carlo (DMC) [16, 17] techniques for the smaller aggregates, while for larger systems (N≥100) the full quantum mechanical approaches are still largely out of reach. Even approximate methods are difficult to implement due to their computational cost, so that simplifying assumptions have to be made in order to extend the analysis to the larger aggregates.

Global optimization of the bound structure energetics can provide a suitable alternative to overcome such difficulties, a reason why this technique may play a role in the determination of the geometries of a wide variety of systems, such as proteins, crystals and clusters [18]. However, it also becomes an extremely costly task as the number of atoms increases due to the exponential growth of the local minima of comparable value: a great deal of effort has therefore gone into developing efficient methods to find the lowest energy structures of molecular clusters [19].

The interest on the interaction between alkali metal atoms (Li, Na, K) and rare gas atoms has also been renewed due to recent experiments measuring the index of refraction of an atomic matter wave passing through a dilute medium of rare gas atoms [20]. Clusters composed by lithium and helium atoms therefore constitute systems amenable to testing the effect of intermolecular interactions on their structure since modern ab-initio and model potential calculations are expected to provide accurate descriptions of these interactions forces owing to the small number of electrons involved in their description. Experimentally, the alkali atom can be added to the initial helium droplet by taking advantage of the ease with which these aggregates can pick up one or more of such impurities [21], while the advent of the more recent transmission grating observations have opened the possibility to investigate the relative stability of weakly bound clusters up to a few tens of helium atoms [22].

When ionization occurs, there is still a considerable lack of realistic microscopic information about the solid order thought to be originated by the presence of the ion [23] and a limited description of its dependence on the chemical features in the case of molecular ionic dopants. In the case of $A_2^+(He)_n$ (A=Li, Na and K) the occurrence of much deeper attractive wells with respect to neutrals, together with the effect of the potential anisotropy, is expected to lead to substantially different structures when compared with the neutral

counterparts.

The aim of this work is therefore that of employing a genetic algorithm approach for the study of the ground state of $A_2^+(He)_n$ clusters, an approach which relies on the energy optimization on the global potential energy surface of the cluster.

There are obviously questions related to such an approach in relation to the quantum nature of the nanoaggregates where Van der Waals (VdW) forces are expected to dominate the interaction landscape. Thus, we have analyzed in the past the reliability of a classical picture for describing ionic dopants in a quantum solvent like bosonic He [24, 25, 26] and found that the presence of the stronger ionic interactions drives the overall stability of the smaller aggregates and causes two chief effects in such systems, as already mentioned before (i.e. electrostriction and snowballs), which contribute to confirm the classical results.

Furthermore, the selection of a simplified description of the overall interaction which we model via the sum-of-potentials (SOP) scheme

$$V(\mathbf{R}, \mathbf{r}) = \sum_{i=1}^{N} V_{\text{He}-\text{M}}(\mathbf{r}_i) + \sum_{ij} V_{\text{He}-\text{He}}(\mathbf{R}_{ij}) \ , \tag{1}$$

where the vectors $\mathbf{r}_i$ label the interactions between each ^{4}He solvent atom and the dopant molecule M, while the $\mathbf{R}_{ij}$'s describe the distances between the helium adatoms within each cluster of size N, allows us to immediately relate the features of the component two-body (2B) potentials with the behavior of each cluster as a function of its size.

In the present systems, as done before by us [27], we have included an additional correction to account for the effects due to many-body (MB) forces. The latter, however, are found not to change the overall pattern of structural evolution produced by the SOP scheme while slightly changing the actual energy values.

The paper is organized as follows: in Section II the method and the potential energy surface employed in this work are briefly reviewed while in Section III we present the main results obtained on the energetics and the spatial distributions. Finally, in Section IV our conclusions are summarized.

II.   THE THEORETICAL MACHINERY: AN OUTLINE

To obtain an analytical expression for the total cluster energy, we start by adding only the contributions coming from the impurity-helium [27] and helium-helium potentials [28],

thereby initially neglecting the many-body effects present in the clusters and following the SOP scheme of eq. (1). A large number of previous studies have been devoted to the evaluation of the leading three-body contributions to interaction potentials between several complexes and noble gas atoms (see for instance our work [29] and references therein), since besides their contributions to the binding energy, three-body terms may in principle influence the geometry of the cluster. In spite of their limited importance found by our previous calculations on this type of systems [24, 25, 26], we have incorporated them through the procedure described below.

The chief reason why such many-body effects remain fairly small in comparison with the total energy [25, 26, 27, 28, 29, 30] is because of the small polarizability of its closed-shell configuration where no significant changes are expected to occur in the electronic structure of helium atoms due to the presence of the ionic impurity. Thus, the only MB correction that we have considered in our calculations is the coupling between the dipole moments induced by the cation on the electron density of a pair of helium atoms. The analytical formula for this term is very simple once we consider a point charge located at the center of mass of the molecular ion, and is given by

$$V_{3B}(r_{ij}, r_i, r_j) = -\frac{\mu_i \mu_j}{r_{ij}^3} \left[2 \cos \vartheta_i \cos \vartheta_j - \sin \vartheta_i sin \vartheta_j \right] \ , \qquad (2)$$

where the angles are formed between each dipole distance from the point like charge (r_i, r_j) and the line joining them (r_{ij}). Each dipole moment μ_i can then be evaluated via the well-known formula: $\mu_i = \alpha/r_i^2$, α being the He polarizability.

The interactions between each solvent atom and the molecular dopant has been the subject of previous studies in our group, where the He-A_2^+ anisotropic potential energy surfaces have been evaluated with the ionic core molecular bond kept at its equilibrium value [27].

The relevant features of the intermolecular potentials associated with a single ^{4}He atom can be appreciated by looking at the data of figure 1: the strongly anisotropic character of the angular dependence of the PES is clearly seen for all the three dimer ions. The absolute minima for the three PESs are collinear while they also present an angular saddle in the C_{2v} geometry, where each potential is much less attractive. The maximum well depths are -380, -95 and -37 cm^{-1} for Li$_2^+$, Na$_2^+$ and K$_2^+$ respectively.

In the same figure we report also the He-He potential: its relative strength with respect

to the He-ion one has an important influence on the growth of the cluster: as we will show below, since Li_2^+-He is the strongest interaction, the collocation of the He adatoms will occur on both sides of the molecule almost independently. In the case of K_2^+, instead, the less attractive ion-He interaction is not able to balance the weak He-He potential and the adatoms prefer to arrange themselves asymmetrically on the two linear and equivalent well regions.

The details of the minimization method has been given previously [31] and therefore we will not repeat them here: in what follows we will only outline our present approach. The classical optimization is based on the well-known genetic algorithm [19, 32], a procedure which can provide a reasonably fast route to finding the minima for a general function. The method employed in the present study follows closely the scheme described in ref. [19].

In spite of the marked localization effects of the He adatoms of the inner shells which is caused by the ionic dopant [33], the quantum nature of the present solvent should also be considered when analyzing the final spatial structures. We take into account such effects by substituting the δ functions of the classical picture of atomic network locations by finite spread distributions along the radial variables. A Gaussian function is thus employed to simulate the zero point vibrations of each cluster particle. As a consequence of it, the corresponding radial densities can be approximated through the following expression:

$$\rho(r) = N \sum_{i=1}^{N} \frac{1}{\sqrt{(2\pi\sigma_i^2)}} \exp\left(-\frac{(r-\bar{r}_i)^2}{2\sigma_i^2}\right) \tag{3}$$

where σ_i is chosen as the product of the standard deviation of the quantum ground vibrational state of the Li_2^+-He system, already computed earlier by us [27], and the uncertainty on the radial values obtained from the η_j^i parameters of the genetic algorithm. The r_i is the i-th atom distance from the center-of-mass of the impurity after optimization. This analysis allows us to obtain spread distributions for the clustering of the *classical* He atoms around the dopant ion, hence by somehow including quantum delocalization effects for the adatoms near the ionic dopant.

We shall see below how such corrections do includes delocalization but follows qualitatively the finding from the classical description provided by our optimization scheme, the latter being however much more helpful in describing spatial collocations of the solvent atoms within the shells closer to the ionic dopants.

III. ENERGETICS AND STRUCTURES

The presence of long-range polarization forces causes the effects of the impurity-helium interactions to extend over a considerable amount of solvent atoms within the cluster structure. We have therefore analyzed a broad range of cluster sizes for a nonvibrating molecular partner in order to unravel such effects in the title systems and to relate them to their specific interaction potentials.

To begin with, we report in figure 2 the single-atom evaporative energies which are defined as:

$$\Delta E_N^{(1)} = E_{N-1} - E_N \ . \tag{4}$$

For all the three type of clusters we see some interesting features. The pronounced steps appearing in the evaporation energy in the small cluster range are a signatures of the completion of some solvation sub-shells, while the peaks are imprints of the appearance of particularly stable structures (magic numbers). For larger clusters those energies present a slightly oscillatory pattern as additional helium atoms are added during the system's growth: the mean value is approximately 50 cm^{-1} for all the three systems. The K$_2^+$(He)$_N$ case however, does not show any clear indication of completion of a solvation shell, but only of some "magic" numbers appearing at N=6, 12, 17, and 24. For the Na$_2^+$ case we do see the filling of the first shell with 6 adatoms and a magic number at N=20. In the case of the Li$_2^+$ the structuring of the first shell is evident at N=6 and three small peaks at N=14, 16, 18 are signatures of additional stable species. It is worth pointing out here that for both sodium and lithium ionic dimers the first two He atoms are strongly bound to either sides of the impurity as independent partners.

These effects are even more clearly appreciable in the behavior of the second energy differences reported by figure 3. This indicator measures the stability of each cluster with respect to the nearest ones and is useful for the detection of shell structures or of "magic" numbers when observing cluster growth. It is defined as

$$\Delta E_N^{(2)} = E_{N+1} + E_{N-1} - 2E_N \ . \tag{5}$$

The data reported in figure 3 confirm substantially our previous findings in terms of magic numbers.

From the data related to the intensive quantity E$_N/N$ and reported in figure 4 only for

the Li-doped species, one can see that the average energies for Li_2^+ (open circles) tend to reach an asymptotic value of about 75 cm^{-1} as the cluster size increases. Beyond this value, in fact, the inclusion of any new adatom to the cluster produces almost the same effect on the energetics. On the other hand, it is clear from the initial values of this quantity that only the first two ^{4}He adatoms can be regarded as truly independent partners while the additional ones, although still strongly bound to the cation, show the helium-helium interactions important role in reducing the incremental contributions of sequential adatoms in the small and intermediate cluster sizes. It is interesting to compare such data with similar calculations for ^{4}He clusters containing the cationic monomer Li^+ as a dopant [34]; they yield the E_N/N values reported in the same figure 4 by open triangles. The number of solvent atoms which attach to the Li^+ ion in a nearly independent manner is now 6 while, on the other hand, we clearly see the same overall trend as that shown by the dimer in terms of changes of the E_N/N binding energy as N increases: the latter quantity is progressing towards an asymptotic value as in the dimer case. In the larger clusters of both species the adatoms will view the dopant essentially as a localized, point-like positive charge.

Another way of looking at the solvation process described by our classical calculation is to consider the "normalized" total and evaporation energy: we report in figure 5 the classical minima energies divided by the D_e of the single He moiety. In the inset we also show the slope of such quantities with respect to N. The growth of the cluster for Li_2^+ and Na_2^+ is clearly marked by the existence of a 6-atom shell and by an almost constant rate of energy acquisition during the accretion process. Above $N = 6$, for Li_2^+ and Na_2^+ the rate of increase in binding energy is of about $0.2 D_e$ and $0.4 D_e$ respectively for each He atom. The case of K_2^+, on the other hand, does not show any special structuring at $N = 6$ and the rate of increase in energy is $1.0 D_e$, a value which shows a behavior analogous to that of a pure He cluster, albeit on a different scale, where the same energy is gained for each adatom attached to the others. We conclude that, despite being a cationic molecular ion, the solvation process around K_2^+ behaves as if it were one of the equivalent He atoms so that from an energy point of view, its role is not different from any other adatom in the cluster.

A.   A selection of clusters' geometries

The geometries of the optimized clusters for Li_2^+, Na_2^+ and K_2^+ for N=2, 4 and 6 are shown in figure 6. The pictorial story told by that figure clearly indicates that for the Li_2^+ case the solvation proceeds symmetrically at the two ends of the molecule. On the other hand, in the Na_2^+ the resulting structures are less symmetric because of the competing energy gain coming from forming He-He networks on one side of the molecular ion. For the case of K_2^+ the He atoms prefer to locate themselves on one side only: this is obviously due to the weakening of the dimer-He interaction which then becomes competitive with the He-He potential giving rise to the preferential formation of the mentioned He-He networks.

Figure 7 further shows a selection of optimized geometries for the larger clusters: we see that triangular, tetrahedral and planar configurations are formed almost independently around each cationic center. The dominance of linear wells in the Li_2^+-He interactions pushes the sequential adatoms to be collocated in them as close as possible to each other so that the two nearly independent microsolvation *cages* grow around each of the Li atoms in the Li_2^+ dimeric cation. This independence effect does not occur for clusters which contain Na_2^+ and K_2^+ as dopants since, due to their weaker interactions with each solvent atom, experience a marked competition with the clustering process of He atoms.

B.   The quantum effects

In order to provide an estimate of the quantum effects due to delocalization and ZPE, we have performed accurate Variational and Diffusion Montecarlo calculations on the smaller moieties containing all the three species. The method has been extensively given before by us [33] and therefore will not be described again in the present work. We report in Table I the quantum energies (D_0), the classical minima (D_e) and the ZPE %.

As can be seen from the data reported in Table I, and especially from those in its last column, the quantum results substantially confirm the picture of an independent growth of the cluster around the two sides of the molecule (see for comparison figure 5). The ratios $D_0(N)/D_0(1)$ for Li_2^+ and Na_2^+ are in fact consistent with the classical result of a symmetric building process which accommodates two atoms by the two molecular sides and then continues building the cluster by alternatively placing the second and the third

N	$D_0(N)$	$D_e(N)$	%ZPE	$D_0(N)/D_0(1)$
		Li_2^+		
1	-254.081 ± 0.035	-380.945	33.0	1.0
2	-515.750 ± 0.130	-761.781	32.3	2.0
3	-639.104 ± 0.800	-994.777	35.7	2.5
4	-895.998 ± 0.100	-1227.588	27.0	3.5
		Na_2^+		
1	-49.462 ± 0.340	-95.026	47.9	1.0
2	-98.334 ± 0.120	-190.033	48.2	2.0
3	-127.810 ±0.056	-254.476	49.8	2.6
4	-151.076 ±0.120	-322.083	53.1	3.0
		K_2^+		
1	-17.470 ± 0.056	-37.41	53.3	1.0
2	-35.020 ±0.073	-75.01	53.3	2.0
3	-47.930±0.149	-119.40	59.9	2.7
4	-60.770 ±0.188	-156.80	61.2	3.5

TABLE I: Classical (D_e) and quantum (D_0) binding energies for the smaller clusters. All energies in wavenumbers.

atom. The quantum results for K_2^+ are however different from our classical findings since the quantum solvation seems to proceed symmetrically when correctly including quantum effects. This is related to the large ZPE values existing in $\mathrm{K}_2^+(\mathrm{He})_n$ which therefore makes more stable the symmetric structures such as $N = 4$ with an even number of adatoms.

In order to also account for the effects of delocalization on the classically optimized structures, we report in figure 8 the radial distributions of the helium atoms on both sides of the molecules. We have generated such distributions starting with the classical results while the final, "quantum" distributions have been obtained from eq. (3) using the standard deviation inferred from a ground state DVR wavefunction for the impurity-He system as discussed in our earlier work [27]. Since the solvation cage is often asymmetric with respect to the two end of the cationic dimer, we have counted the number of particles of each side of the molecules and we have normalized the left-hand and right-hand side of the density

accordingly.

As we can see in figure 8, the $Li_2^+(He)_N$ clusters are almost symmetric (for an even number of He atoms) up to $N=18$, the Na_2^+ doped ones have both symmetric and asymmetric geometries. Finally the K_2^+ doped clusters have clearly asymmetric spatial arrangements.

IV. CONCLUSIONS

The data reported in this work have focused on the energetics and the spatial collocations of solvent atoms in ^{4}He droplets doped by three different cationic dimers: Li_2^+, Na_2^+ and K_2^+.

The interactions within the clusters have been obtained by a sum of the two-body potentials acting between its components and derived from ab initio calculations [27]. A realistic approximation to the three body term has also been included in the energy expression to evaluate its effects which have turned out to be rather small.

The optimization procedure we have employed here is based on a genetic algorithm scheme already discussed by us before [30, 31] and the optimized structures have been analyzed in terms of their geometric features in order to explain the increased asymmetry of the solvation shells around the cationic dimer when going from Li_2^+ to K_2^+ as dopants.

The following characteristics were found to occur along the series of the examined clusters: in the clusters doped by Li_2^+ and Na_2^+, the interaction between each He atom and the ion is much stronger than the He-He potential and therefore causes the formation of quasi-linear accumulation cages of solvent atoms with respect to the molecular dopants. The initial solvent particles thus start to place themselves at the two ends of the molecule and far away from each other, thereby creating an initial subshell of 6 atoms. Adding more He atoms makes the two parts of this subshell grow in an independent fashion by collocating solvent atoms alternatively on either of the two sides of the dimer.

The present study, therefore confirms the expected dominance of ionic forces in driving cluster shapes when the dopant is a cationic molecule and clearly shows the crucial role played by changing the competitive strength of the ion-He interaction with respect to the He-He network of interactions. Thus, for the K_2^+ dimer we found that the construction of the solvent cage is asymmetric and dominated by the He-He network formation. For Li_2^+ and Na_2^+, on the other hand, we have shown that a rigid *snowball* structure is formed as a regular configuration within the first shell that encloses the solvated cation (with $N=6$),

followed by more delocalized collocations of the solvation atoms for clusters beyond that size. Such collocations are largely creating symmetric solvent cages at the two ends of each ionic dimer.

In spite of using a classical representation of the solvent atoms, we have shown that for ionic molecular dopants (as it has occurred with atomic ions [24]) the final description of the microsolvation process in the smaller He clusters turns out to be keeping with the quantum results and indicates the present approach as providing useful insights on that process.

[1] J. P. Toennies and A. F. Vilesov, Ann. Rev. Phys. Chem. 49, 1 (1998).

[2] J. P. Toennies, A. F. Vilesov, and K. B. Whaley, Phys. Today 54, 31 (2001).

[3] F. Stienkemeier and A. F. Vilesov, J. Chem. Phys. 115, 10119 (2001).

[4] J. P. Toennies and A. F. Vilesov, Angew. Chem. Int. Ed. 43, 2622 (2004).

[5] F. Stienkemeier and K. K. Lehmann, J. Phys. B 39, R127 (2006).

[6] A. Buchachenko, N. Halberstadt, B. Lepetit, O. Roncero, Int. Rev. Phys. Chem. 22, 153 (2003)

[7] A. García-Vela, J. Chem. Phys. 108, 5755 (1998)

[8] P. Slavicek, M. Roeselova, P. Jungwirth, B. Schmidt, J. Chem. Phys. 114, 1539 (2001)

[9] N. Runeberg, M. Petterson, L. Khriachtchev, J. Lundell, M. Rasanen, J. Chem. Phys. 114, 836 (2001)

[10] G. Frenking, D. Cremer, Struct. Bonding (Berlin) 73, 17 (1990)

[11] K. P. Atkins, Phys. Rev. 116, 1339 (1959)

[12] P. Claas, S. O. Mende, F. Stienkemeier, Rev. Sci. Instrum. 74, 4071 (2003)

[13] M. W. Cole, R. A. Bachman, Phys. Rev. B 15, 1388 (1977)

[14] M. W. Cole, F. Toigo, Phys. Rev. B 17, 2054 (1978)

[15] M. Casalegno, M. Mella, G. Morosi, D. Bressanini, J. Chem. Phys. 112, 69 (2000)

[16] W. Topic, W. Jager, N. Blinov, P.-N. Roy, M. Botti, and S. Moroni, J. Chem. Phys. 125, 144310 (2006)

[17] F. Paesani, F. A. Gianturco, J. Chem. Phys. 116, 10170 (2002)

[18] J. Hernández-Rojas, D. J. Wales, J. Chem. Phys. 119, 7800 (2003)

[19] M. Iwamatsu, Comp. Phys. Comm. 142, 214 (2001)

[20] J. Vigue, Phys. Rev. A 52, 3973 (1995)

[21] A. Scheidermann, J. P. Toennies, J. A. Northby, Phys. Rev. Lett. 64, 1899 (1999)

[22] W. Schollkopf, J. P. Toennies, J. Chem. Phys. 104, 1155 (1996)

[23] W. I. Glaberson, W. W. Johnson, J. Low Temp. Phys. 20, 313 (1997)

[24] C. Di Paola, F. Sebastianelli, E. Bodo, I. Baccarelli, F. A. Gianturco, M. Yurtsever, J. Comp. Theor. Chem. 1, 1045 (2005)

[25] C. Di Paola, F. A. Gianturco, Eur. Phys. J. D 35, 513 (2005)

[26] E. Bodo, F. Sebastianelli, F. A. Gianturco, E. Yurtsever, M. Yurtsever, J. Chem. Phys. 120, 9160 (2004)

[27] E. Bodo, E. Yurtsever, M. Yurtsever, F. A. Gianturco, J. Chem. Phys. 124, 074320 (2006)

[28] K. T. T. U. Kleinekathofer, J. P. Toennies, C. L. Yiu, Chem. Phys. Lett. 249, 257 (1996)

[29] I. Baccarelli, F. A. Gianturco, T. González-Lezana, G. Delgado-Barrio, S. Miret-Artés, P. Villareal, J. Chem. Phys. 122, 144319 (2005)

[30] F. Marinetti, E. Bodo, F. A. Gianturco, J. Comp. Theor. Chem. 5, 543 (2006)

[31] F. Marinetti, E. Bodo, F. A. Gianturco, Chem. Phys. Chem. 8, 93 (2007)

[32] T. Back, H.-P. Schwefel, Evol. Comput. 1, 1 (1993)

[33] e.g. see: E. Coccia, E. Bodo, F. Marinetti, F.A.Gianturco, E. Yurtsever, M. Yurtsever, E. Yildrim, J. Chem. Phys.,126, 1 (2007).

[34] F. Marinetti, E. Coccia, E. Bodo, F. A. Gianturco, E. Yurtsever, M. Yurtsever, E. Yildrim, Theor. Chem. Acc. (2007) (published on line).
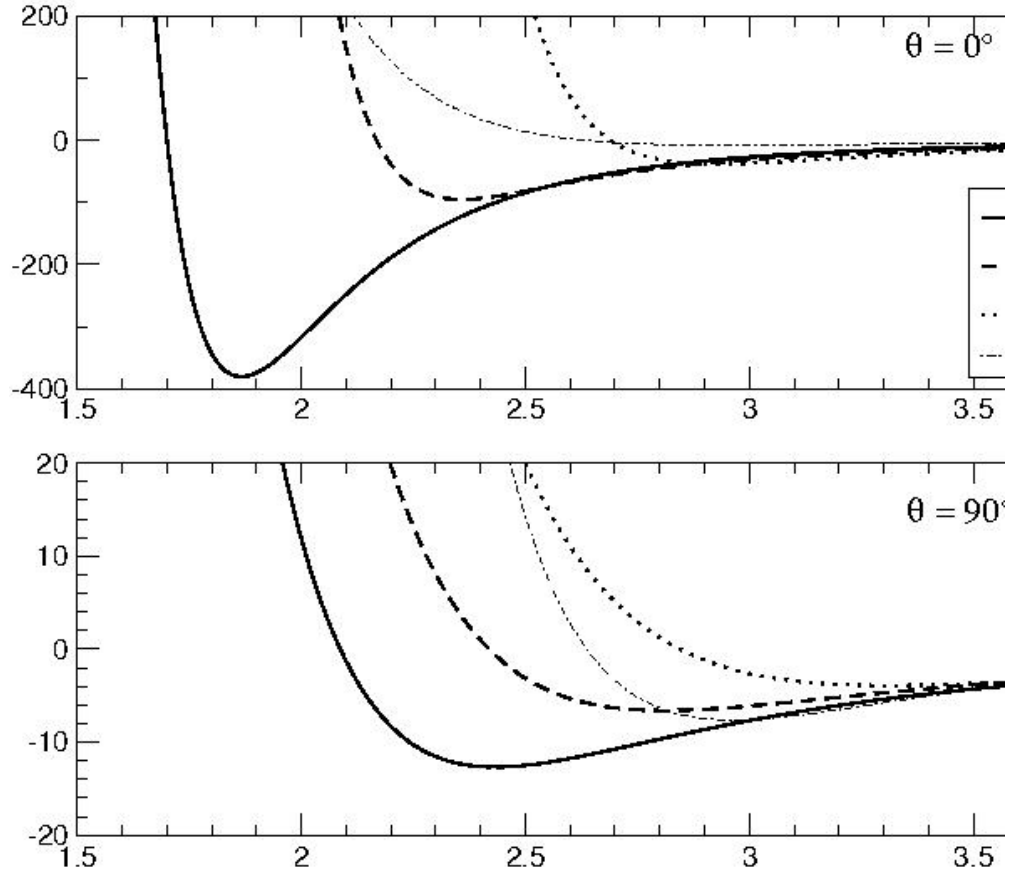
FIG. 1: A_2^+-He interaction as obtained from the ab initio calculations of [27]: units in Åand cm^{-1}. The dash-dotted line is the He-He potential from ref [28]
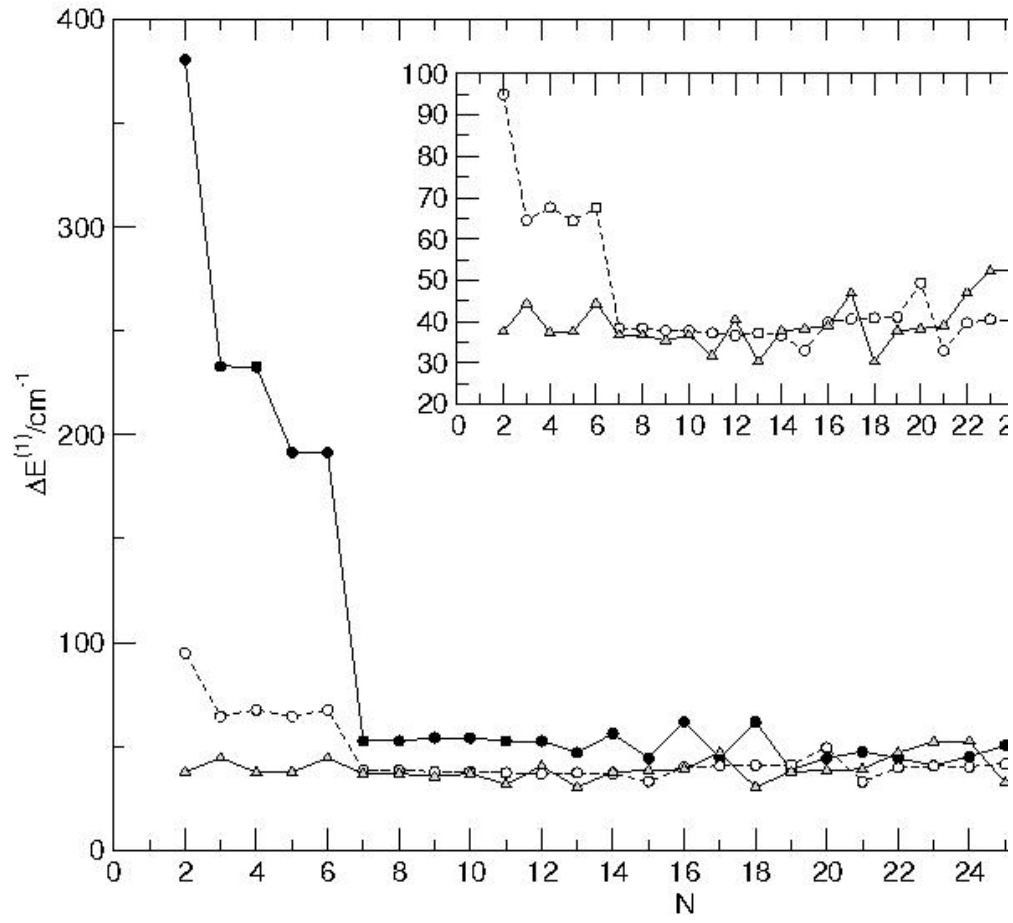
FIG. 2: Computed evaporation energies of the helium clusters with the three cationic dopants.
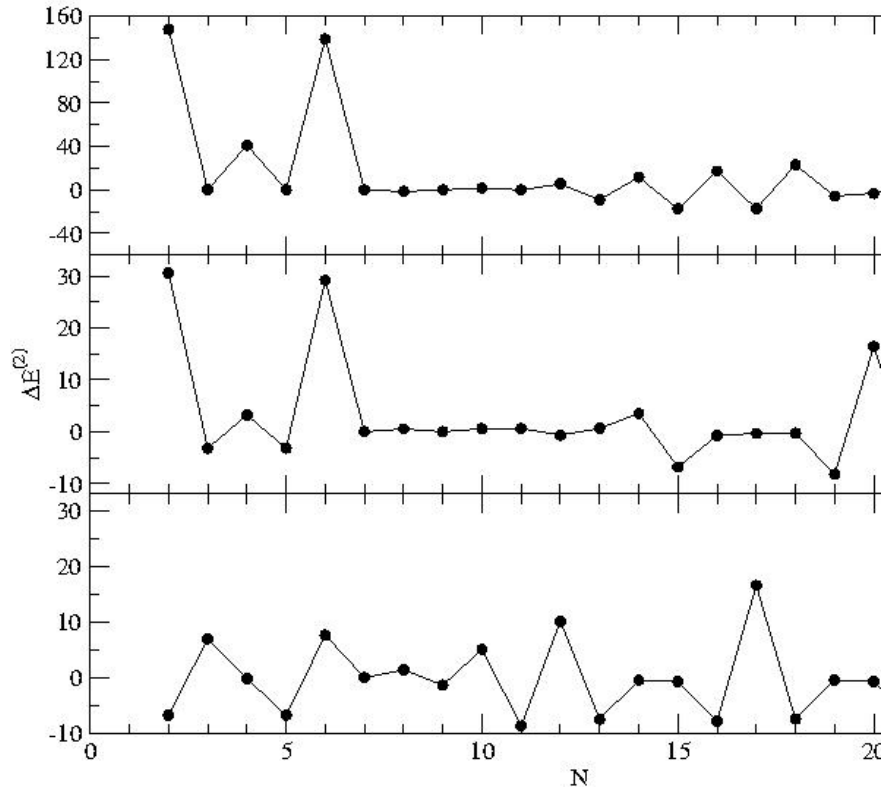
FIG. 3: Computed 2nd order differences for the three alkali-metal ionic dimers as functions of the no. of He atoms in the clusters.
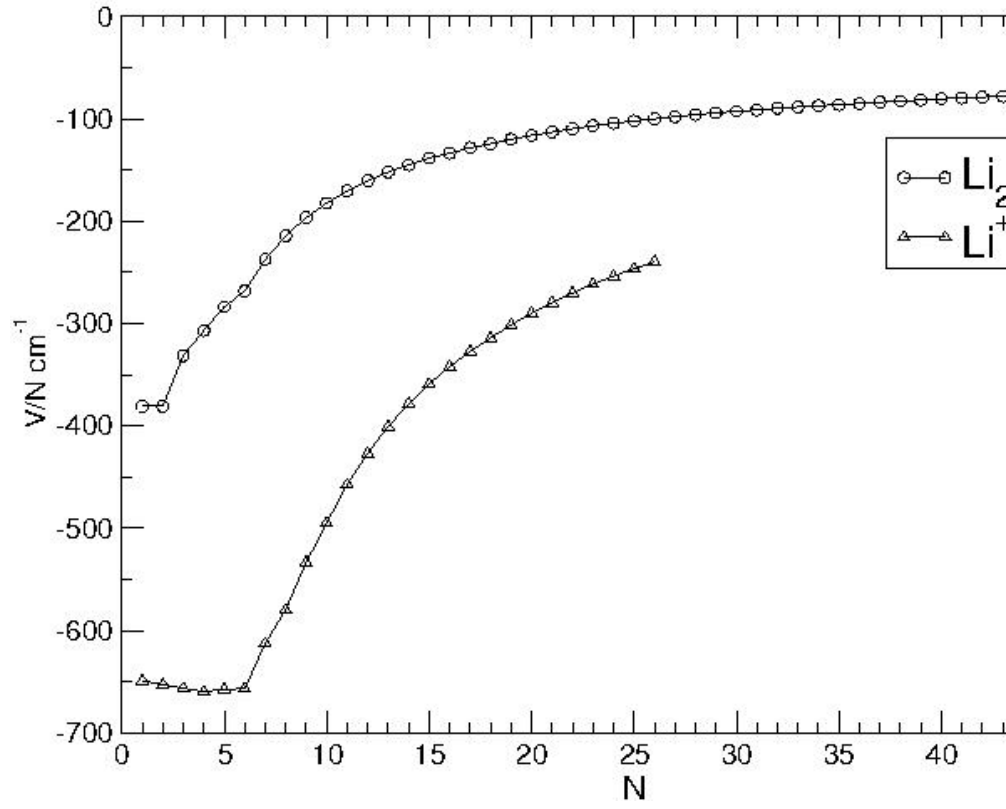
FIG. 4: Computed average energy per added solvent atom. The calculations for Li$^+$ are reported in ref. [34]).
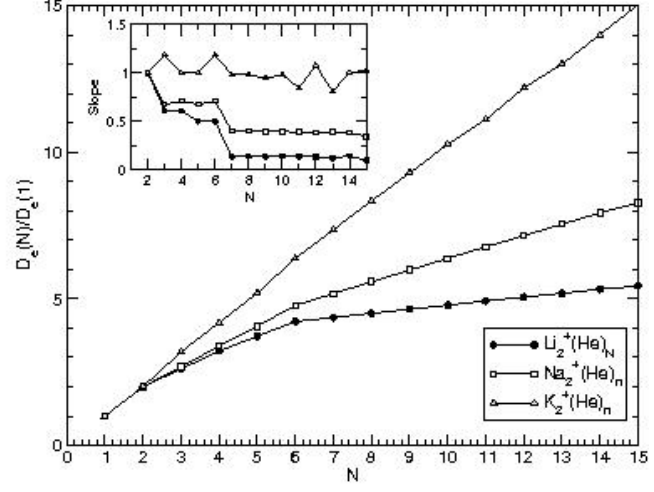
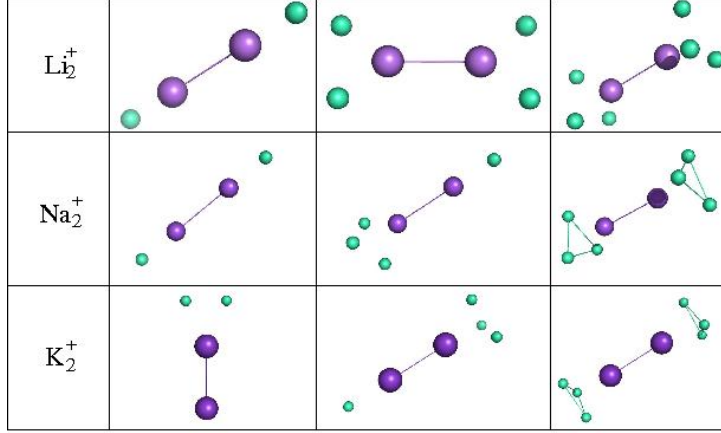FIG. 5: $D_e(N)/D_e(1)$ ratios for the three dopant species.

FIG. 6: Optimal spatial structures of the clusters of Li_2^+, Na_2^+ and K_2^+ for N=2, 4, 6. The darker, larger spheres represent the cationic dopant.
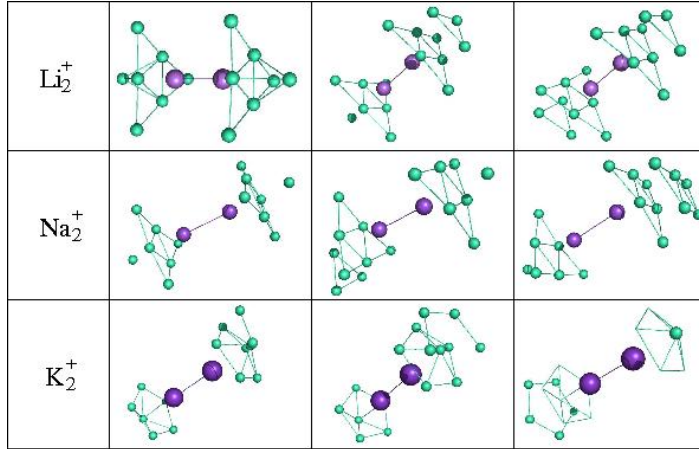

FIG. 7: Structures of the optimized geometries for the $A_2^+(He)_N$ clusters with N=14, 16, 18.
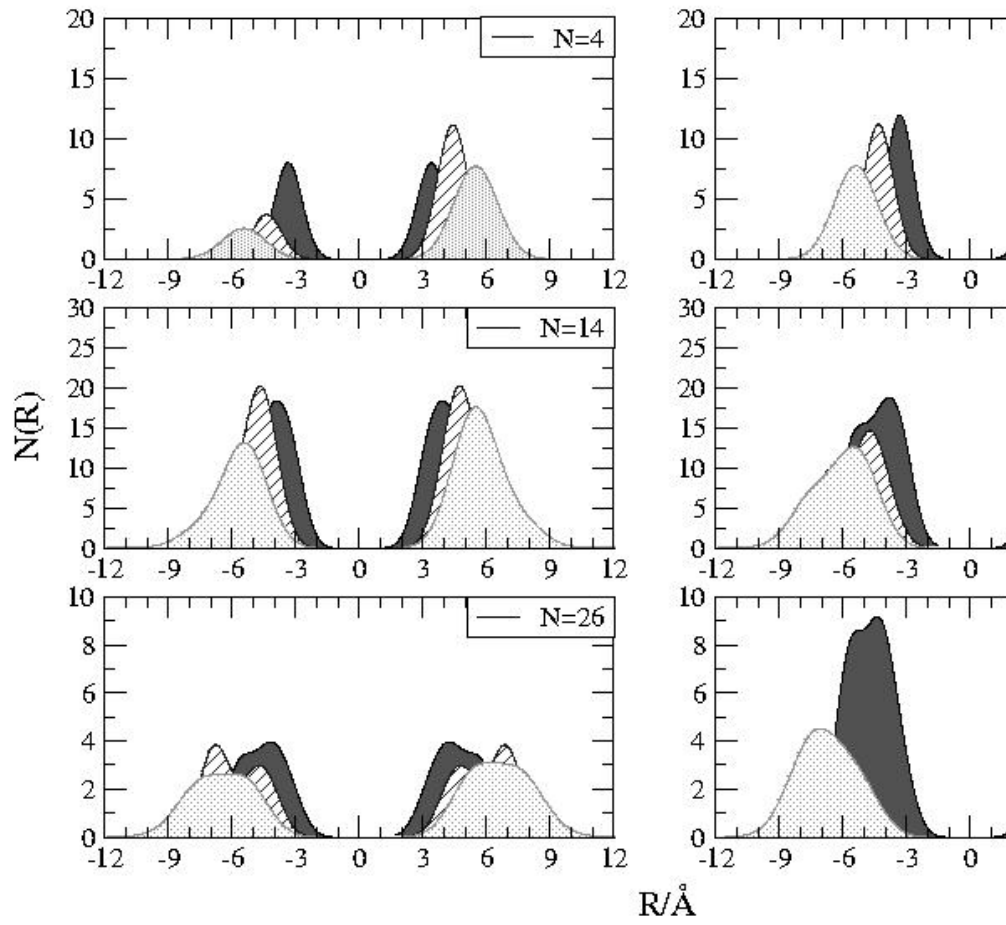
FIG. 8: Computed radial distributions of solvent atoms from the dopant's center-of-mass for different cluster sizes. Li_2^+, Na_2^+ and K_2^+ distributions are represented by the differently shaded areas: dark for Li_2^+, lines for Na_2^+ and gray for K_2^+.